Original Article

Dosimetry of ^{175}Ytterbium-poly (amidoamine) Therapy for Humans' Organs

Navideh Aghaei-Amirkhizi[1,2], Sodeh Sadjadi[3], Leila Moghaddam-Banaem[3], Mitra Athari-Allaf[1], Fariba Johari-Deha[2]

[1]Department of Medical Radiation Engineering, Science and Research Branch, Islamic Azad University, [3]Department of Production and Separation of Isotopes, Nuclear Material and Fuel School, Nuclear Science and Technology Research Institute, [2]Department of Radiopharmacy and Radioisotopes Research, Applied of Radiation School, Nuclear Science and Technology Research Institute, Tehran, Iran

Abstract

Purpose: This investigation focuses on biodistribution of irradiated dendrimer encapsulated ytterbium-175 (^{175}Yb) and to estimate the absorbed dose from intravenous injection of PAMAM encapsulated ^{175}Yb to human organs. **Methods:** A dendrimer compound containing an average of 55 Yb^{+3} ions per dendrimer was prepared and irradiated with neutrons for 2h at 3×10^{11} n.cm^{-2}s^{-1} neutron flux. The resulting mixture was injected into a group of tumor bearing mice and the mice were excised, weighed and counted at certain times to study the biodistribution. The human organs absorbed dose was assessed by MIRD schema and MCNP simulation. **Results:** The specific activity and radiochemical purity of the irradiated nano-composite were 7MBq/mg and >99% respectively. The rapid up take of dendrimer was in liver, lung, and, spleen. MIRD and MCNPX were applied for dose estimation. The human absorbed dose in liver, lung, spleen, kidney and bone that simulated by MCNP are 1.266, 0.8081, 0.8347, 0.03979 and 0.01706 mGy/MBq respectively and these values for MIRD schema are 1.351, 0.73, 1.03, 0.039, and 0.0097 mGy/MBq respectively. **Conclusion:** The results showed that ^{175}Yb-PAMAM nano-radiopharmaceutical has potential of application for liver and lung tumors.

Keywords: Ytterbium-175, dosimetry, MCNP, medical internal radiation dosimetry, nano-radiopharmaceutical, poly (amidoamine)

Received on: 13-01-2018 **Review completed on: 07-07-2018** **Accepted on: 22-08-2018**

Introduction

Nano radiopharmaceutical therapy (NRPT) is a new method for solid tumor therapy. The treatment uses a radioactive form of radionuclide encapsulated in the poly amidoamine dendrimers.[1] The poly (amidoamine) (PAMAM) dendrimers have attracted attentions for cancer treatment by their characteristics of targeted drug carriers, delivery agents, and imaging agents in human systems.[2-5] Dendrimers have shown robust stability and being structurally and chemically well-defined templates, they are capable to conjugate with metals. Recently, PAMAM dendrimer-based multifunctional cancer therapeutic conjugates have been designed and synthesized in pharmaceutical industry.[6,7]

The beta emitter radionuclides help to destroy solid tumor cells and are favorable because of their short path length that enables to avoid irradiation of normal tissues. Researchers have reported successful encapsulation of radionuclides such as ^{177} Lu, ^{212}Pb, ^{166}Ho, and also alpha-emitting daughter radionuclide ^{212}Bi, for NRPT application.[8-10]

Access this article online

Quick Response Code:

Website: www.jmp.org.in

DOI: 10.4103/jmp.JMP_8_18

We have reported the preparation of dendrimer-encapsulated Ytterbium-175 (^{175}Yb) radio-nanoparticles and its biodistribution in tumor-bearing rats.[11] ^{175}Yb ($T_{1/2}$=4.2 days), with a β- emission (E_{max} 479keV and 86.5% yield), decays to stable ^{175}Lu. Following this decay γ photons of 113 keV (1.9%), 282keV (3.1%), and 396 keV (6.5%) are emitted which are appropriate for imaging. These physical characteristics render ^{175}Yb as a suitable radionuclide for developing theranostic agents using its β- emission for

Address for correspondence: Dr. Leila Moghaddam-Banaem, Department of Production and Separation of Isotopes, Nuclear Material and Fuel School, Nuclear Science and Technology Research Institute, End of Kargar Street, Tehran, Iran.
E-mail: lmoghaddam@aut.ac.ir
Dr. Fariba Johari-Deha, Department of Radiopharmacy and Radioisotopes Research, Applied of Radiation School, Nuclear Science and Technology Research Institute, End of Kargar Street, Tehran, Iran.
E-mail: fjohari@aeoi.org.ir

How to cite this article: Aghaei-Amirkhizi N, Sadjadi S, Moghaddam-Banaem L, Athari-Allaf M, Johari-Deha F. Dosimetry of ^{175}Ytterbium-poly (amidoamine) therapy for humans' organs. J Med Phys 2018;43:173-8.

therapy and favorite γ photons for carrying simultaneous scintigraphic studies.[12-14]

Dosimetry is required by the clinician for several reasons. First, treatment is often limited by the dose delivered to critical organs, for example, bone marrow. Particular attention is placed on the marrow and kidney as dose-limiting organs. Secondary, dosimetry is required to prescribe the correct activity of radionuclide. Indeed, internal radiation dosimetry of radiopharmaceuticals is an important aspect of nuclear medicine to weigh risk versus benefit considerations and also choosing an appropriate way to spare the surrounding normal tissues from irradiation.[15-18]

Internal dose models and methods in use for many years are well established and can give radiation doses to stylized models representing reference individuals. Kinetic analyses need to be carefully planned, and dose conversion factors that are most similar to the subject in question should be chosen, which can then be tailored somewhat to be more patient specific. Internal dose calculations, however, are currently not relevant in patient management in internal emitter therapy, as they are not sufficiently accurate or detailed to guide clinical decision-making, and as calculated doses have historically not been well correlated with observed effects on tissues. Procedures that utilize ionizing radiation should be performed in accordance with the as low as reasonably achievable philosophy.[19]

For calculating internal dose, we studied the simulation of radiation transport and energy deposition using Monte Carlo N-Particle Transport Code (MCNP) code and Medical Internal Radiation Dosimetry (MIRD). In MIRD method, the dose absorbed in the target organs are estimated by the activities accumulated in the source organ and the S-factors. Many studies have been performed to estimate the organ's activity using MIRD.[20-22]

Another method that recently attracted attention is Monte Carlo which is more precise than other techniques. In radiologic sciences, Monte Carlo techniques have provided much useful information through the simulation of radiation transport. With improved computer technology, more complex Monte Carlo methods may be used in radiation therapy.[17,23]

We reported previously the successful encapsulation of ^{175}Yb by dendrimer.[11] This paper aims at two goals, first acquiring the internal dose of ^{175}Yb-PAMAM in case of entering the radiopharmaceutical in blood circulation and the second comparing dosimetric assessments performed with Monte Carlo codes and MIRD based on the experimental results of biodistribution of dendrimer-encapsulated ^{175}Yb radio-nanoparticles in mice. The results were obtained by MCNP and MIRD were compared in terms of absorbed dose by organs (expressed in mGy per MBq) for liver, kidney, spleen, and lung and other organs. The results of these two studies and the differences are presented in this paper.

Materials and Methods

Materials and instruments

All chemical materials including, Ytterbium (III) oxide, PAMAMG5-NH_2 dendrimer in 5% methanol solution and HNO_3, Sodium borohydride ($NaBH_4$) were purchased from Sigma Aldrich Chemical Co., USA, and Merck, Germany.

Varian Cary3 spectrometer was used for UV-VIS spectra and Philips-CN 30 transmission electron microscope having a point-to-point resolution of 0.23 nm recorded High-resolution transmission electron micrographs. Size distribution data were recorded on a Zetaplus, Zeta potential Analyzer, and Brakhaver for Dynamic Light Scattering. Animal studies were performed in accordance with the United Kingdom biological council's guidelines on the use of living animals in scientific investigations.[24] A high purity germanium detector coupled with a Canberra™ (model GC1020-7500SL) multichannel analyzer on the adjustment of the baseline at 396 keV for the measurement was used for gamma spectroscopy of produced radionuclide, and a dose calibrator ISOMED 1010 (Dresden, Germany) was used for counting distributed activity in mice organs. Radiochemical purity was performed by instant thin-layer chromatography using No-1 Whatman strips.

For biodistribution study 20 female Balb/c mice (18 ± 3 g) with 6–8-week age were purchased from Pasteur Institute of Iran and injected with 4T1 cells to model the cancerous situation for better result in biodistribution of radiopharmaceutical by intravenously injection.

Preparation of nano-radiopharmaceutical of dendrimer-encapsulated metal nanoparticles and biodistribution

The synthesis and production and biodistribution of nano radio-ytterbium described in previous work.[11] Briefly, a 20 mM Yb $(NO_3)_3$ solution was prepared. Then, a 0.01 mM dendrimer solution containing an average 55 Yb^{3+} ions per dendrimer (G5-NH_2 $[Yb^{3}+]_{55}$) was prepared, and pH of this solution was adjusted to 7.5 before to reduction. A 3-fold molar excess of $NaBH_4$ was added to this solution to reduce the dendrimer-encapsulated Yb^{3+} to the zero valent metal G5-NH_2 $(Yb)_{55}$ and its pH was then adjusted to 3, with $HClO_4$ to decompose the excess amount of BH^-_4. The resulting solution (G5-NH_2 $[Yb^{3}+]_{55}$) was purged with nitrogen gas continuously for 20 min and after adding BH^-_4 for reduction, purging continued until 2 h.

The ^{175}Yb-nanoparticles were irradiated with neutron flux of 3×10^{11} n/cm^2/s in Tehran Research Reactor at the pile position for 2 h. The radiochemical purity was performed 24 h after the irradiation by employing ITLC and using 0.1 mM diethylene-triamine-penta-acetic acid chelating agent as the mobile phase to discriminate-free ytterbium from radiolabeled compound.

For biodistribution study, 0.1 mL (7.4 MBq/mL) of radio-nanoparticles solution were injected intravenously through the tail vein. The animals were sacrificed at specified 4, 24, and 48 h time intervals and the specific activity of different organs (blood, heart, lung, adrenal, stomach, intestine, liver, spleen, kidney, muscle, brain, tumor, and bone) were calculated

as the percentage of injected dose per gram of tissue (%ID/g), using gamma detector.

Estimation of human's organs dose

To estimate the absorbed dose by both methods, MCNP and MIRD, cumulated activity in source organs must be calculated. Before calculating the cumulated activity in source organs, a mass correction method (kg/g method) was used to extrapolate biokinetic data from animal model to human by equation (1).[25] The required mass data for the standard adult male of 73 kg were taken from ICRP89.[26]

$$(\%ID)_{human} = \left(\left[\frac{\%ID}{g} \right]_{animal} \times \left[Total - weight_{Kg} \right]_{animal} \right) \times \left(\frac{g_{organ}}{Total - weight_{Kg}} \right)_{human} \quad (1)$$

After obtaining the percentage of injected dose in humans' organs, the activity versus time curves for the source organs including lung, stomach, intestine, liver, spleen, kidney, bone, muscle, and remainder of body in human were plotted. Matlab software was used to calculate the residence times in the source organs by fitting a multicomponent exponential function to these activity-time curves and then the program calculated the values of the amount of activity associated with the component i of the source region (f_i) and the biological elimination constants for the component i, (λ_i) of equation (2). In this equation, λ_p represents the physical decay constant for the radionuclide of interest.[25,27]

$$f_s(t) = f_1 e^{-(\lambda_1+\lambda_p)t} + f_2 e^{-(\lambda_2+\lambda_p)t} + \quad (2)$$

The residence times (τ) in the source organs were obtained by integration of respective fit functions, from t = 0 to t = infinity, after accounting for the physical decay of the ^{175}Yb. Then the cumulative activities in the source organs in MBq-s, were calculated as equation (3), where $\tilde{A}_h$ is cumulative activity in source organ and A_0 is the activity administered to the body at time t = 0, and $f_s(t)$ is the fraction of administered activity present within the source region at time t and (τ) is residence time.[25,27]

$$A_h = \int_0^\infty A_h(t)dt = A_0 \int_0^\infty f_s(t)dt = A_0 \times \tau \quad (3)$$

After obtaining residence time, to estimate the absorbed dose of various organs in human by MIRD method, the $S(r_k \leftarrow r_h)$ that is the so-called S-value, which gives the dose in the region r_k per unit cumulated activity in the source region r_h, was used. The S-values were derived from the set of MIRD tables giving specific absorbed fractions as a function of photon energy of ^{175}Yb in a model of the adult human body and also the absorbed dose of electron energy in source organs were added to obtain the "S" factors in source organs. The S-values for ^{175}Yb were taken from MIRD pamphlet No. 11.[28] The dose calculation and estimation was done for a certain group of organs of human following the MIRD technique as equation (4), in which the absorbed dose, D, to a target organ (r_k) is given. In this equation, $\tilde{A}_h$ is the cumulative activity in the source region r_h and $S(r_k \leftarrow r_h)$ is the S-value.[25]

$$D_{r_k} = \sum_h \tilde{A}_h S(r_k \leftarrow r_h) \quad (4)$$

To simulate the problem with MCNP, an input file that describes the geometry by application of ORNL MIRD man phantom that simulated the whole body, specifies the materials and the source, and defines the desired result from the simulation, must be prepared. The desired result for this study is absorbed doses of vital organs (liver, spleen, lung, and kidney). To calculate absorbed dose using Monte Carlo simulation, either F6 tallies or *F8 tallies can be used, but since ^{175}Yb emits both photons and beta particles, MCNPX was performed once with photon energies and the second time for beta emissions. The F6 tallies, which give results in MeV/g, were converted to Gray (Gy) with the tally multiplier card (FM card). The simulation was done for 10^9 particles, and relative error was decreased to <0.001 for each organ by using variance reduction techniques that includes implicit capture (PHYS). The results of MCNPX are defined for each decay of source material. To convert these results to Gray/MBq of the injected radiopharmaceutical, these outputs of MCNPX for each source organ multiplied in the integration of the surface under the activity versus time curves for the source organs of human (cumulative activity) that explained above.

Results

Figure 1 shows the result of scanning electron microscopy (SEM) of synthesized nanoparticles (a) before irradiation (b) after irradiation by thermal neutron flux. The SEM shows radiation polymerization of the dendrimer. A volume of one PAMAM G5 particle with a diameter in the range of 3–5 nm polymerized to 90 nm after irradiation.

The radiochemical purity was checked during the 120 h after the irradiation, and it is shown in Figure 2. The radiochemical purity was between %97 at 24 h and %86 at 120 h after irradiation. Table 1 and Figure 3 show the biodistribution of nano-radiopharmaceutical at different times in mice, Table 2 and Figure 4 show the extrapolated biodistribution in humans' organs

Table 3 shows the residence time (hour) that obtained from the curves for the source activity in human's organs versus

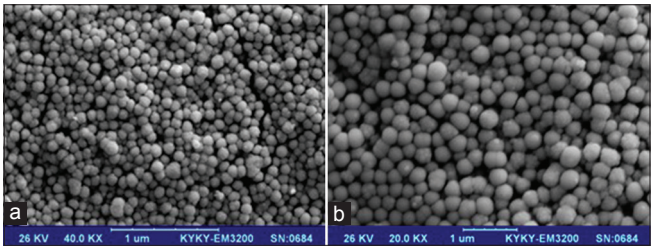

Figure 1: Scanning Electron Microscopy of synthesized nanoparticles (a) before irradiation (b) after irradiation by thermal neutron flux

Table 1: Biodistribution of ^{175}Ytterbium-poly (amidoamine) in mice as percentage of injected dose per gram for each organ (% ID/g)

Organ	4 h	24 h	48 h
Blood	1.976±0.030	0.541±0.027	0.478±0.008
Heart	1.330±0.009	0.437±0.027	0.280±0.004
Lung	9.759±0.083	33.546±0.646	60.456±0.601
Adrenal	0.997±1.635	0.100±1.404	3.693±0.343
Stomach	0.553±0.010	0.129±0.074	0.620±0.213
Intestine	0.781±0.015	0.328±0.112	0.144±0.031
Thyroid	1.144±0.059	0.000±0.182	0.118±0.099
Liver	16.134±0.037	34.608±0.015	43.296±0.065
Spleen	7.735±0.307	17.513±0.616	35.661±0.010
Kidney	1.770±0.268	0.939±0.138	0.868±0.037
Muscle	0.141±0.000	0.211±0.126	0.309±0.588
Bone	1.466±0.093	0.381±0.342	0.987±0.707
Total	1.759±0.152	2.629±0.013	4.080±0.085

Table 2: Human percentage ID/organ by extrapolation of animal data to human (male 73 kg)

Organ	4 h	24 h	48 h
Blood	2.243±0.034	0.772±0.039	0.611±0.011
Heart	0.089±0.001	0.037±0.002	0.021±0.000
Lung	0.989±0.008	4.274±0.082	6.907±0.069
Adrenal	0.003±0.005	0.000±0.005	0.012±0.001
Stomach	0.045±0.001	0.013±0.008	0.057±0.019
Intestine	0.106±0.002	0.056±0.019	0.022±0.005
Thyroid	0.005±0.000	0.000±0.001	0.001±0.000
Liver	5.888±0.013	15.872±0.007	17.807±0.027
Spleen	0.235±0.009	0.669±0.024	1.222±0.000
Kidney	0.111±0.017	0.074±0.011	0.062±0.003
Muscle	0.829±0.000	1.560±0.929	2.050±0.039
Bone	3.121±0.198	1.020±0.915	2.368±0.170
Total	1.759±0.002	2.629±0.000	4.080±0.001

Table 3: The residence times in the source organs

Organ	Residence time (h)
Blood	3.13±0.0159
Heart	0.03±0.0006
Lung	11.89±0.1182
Stomach	0.01±0.004
Intestine	0.033±0.0058
Liver	32.138±0.0063
Spleen	2.093±0.0063
Kidney	0.116±0.0051
Bone	0.883±0.2995
Muscle	3.658±0.2119
Total body	9.190±0.0004

time by integration of the surface under the curves. Table 4 shows the results of MIRD and MCNP and their relative differences. Figure 5 shows the biokinetics of vital organs of human that are extrapolated from animal data. Figure 6 shows the plot of MCNPX for source organs, bone, and soft tissues.

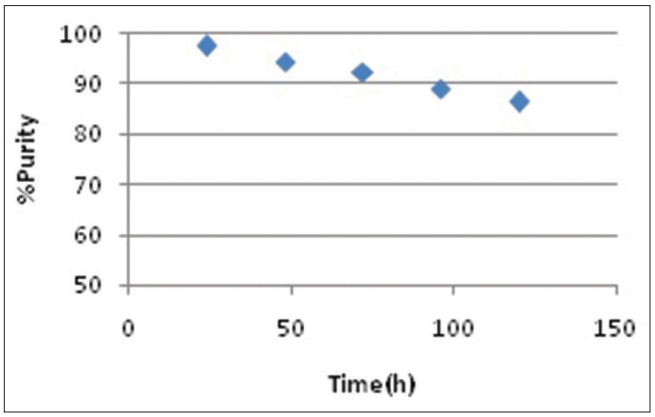

Figure 2: Radiochemical purity of compound during 120 h after irradiation by neutron flux

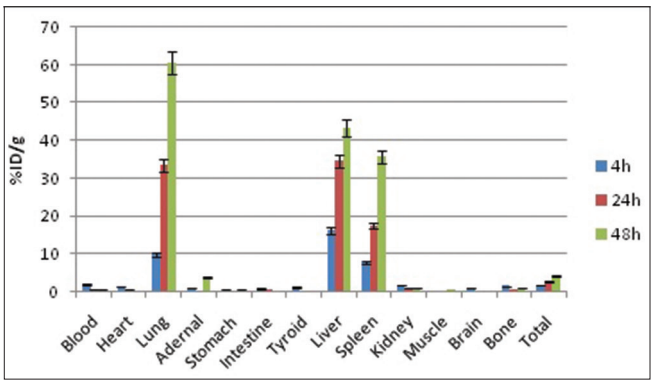

Figure 3: Biodistribution of ^{175}Ytterbium-poly (amidoamine) in mice

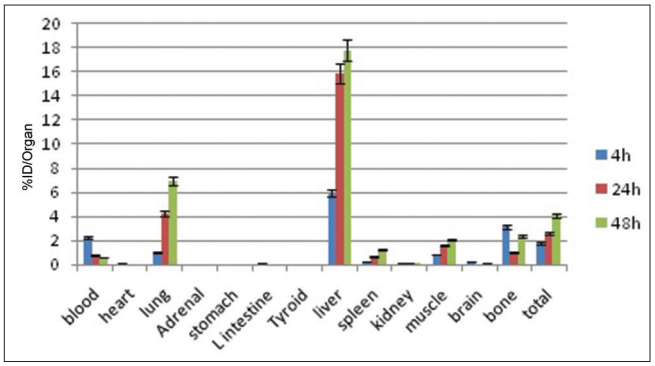

Figure 4: Extrapolation of mice %ID/g to human %ID/Organ

Discussion

Figures 3 and 4 show the biodistribution of the radio-compound after intravenous injection in specified times in mice and the extrapolated data of animal to humans' organs. There is less variation in human organ activities compared to animal data that is because the percentage of human organs to total weight is different with the animal percentage of organs to total weight and in formula 1 this difference can cause the less variation in

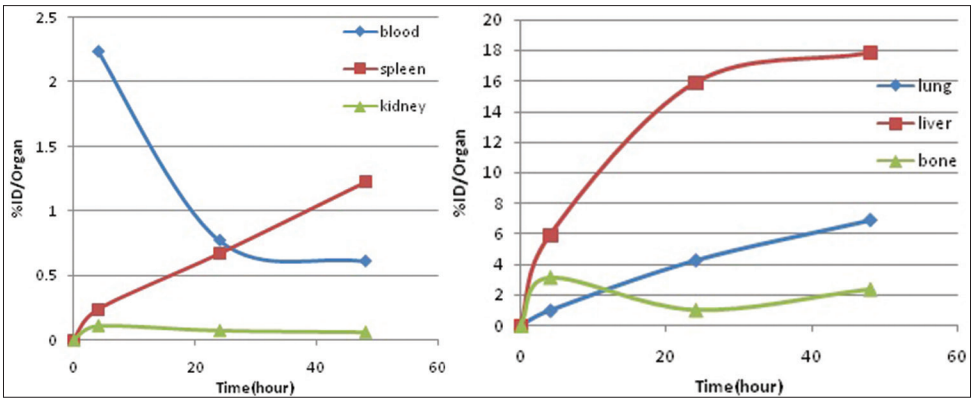

Figure 5: Time–activity curves for human organs that generated from rats data. Initial fast distribution of radiotracer is throughout liver, lung, and Bone, with slower accumulation in blood and spleen. Area under curve is determined by use of MATLAB program by integration of exponential fit

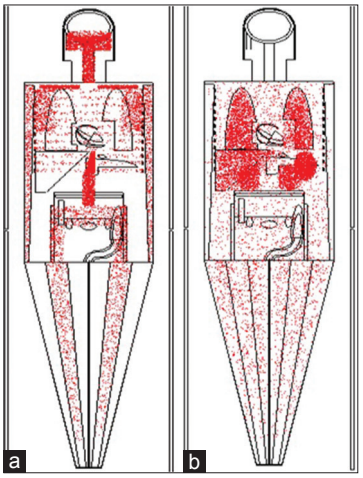

Figure 6: MCNP plot output of source organs, (a) plot of sources on bones (legs, spine, arms, clavicles, rib cage, scapulae, pelvis, skull (cranium and facial skeleton) for 10,000 particles, (b) plot of sources on internal organs and soft tissues including liver, spleen, lungs, kidney, trunk, legs' muscles for 10,000 particles

human organs. The maximum uptakes are in the liver, lung, and spleen. The biodistribution shows the characteristics of nanoparticles such as size and surface hydrophobicity that determine the amount of adsorbed radiopharmaceuticals in organs. The particles larger than 10 μm are located in the lung, and particles between 0.2 and 3 μm accumulate in the liver and spleen, while the small particles (<30 nm) accumulate in a higher concentration in the bone marrow.[29-32]

Figure 5 shows the retention kinetics in various organs that generated from mice data. This figure shows that the initial fast distribution of radiotracer is throughout liver, lung, and bone, with slower accumulation in blood and spleen. The area under these curves is related to cumulative activity in the source organs that used for estimating the absorbed doses.

Table 4 shows the result of 2 methods (MIRD versus MCNPX) and reveals that MIRD underestimate the absorbed dose for bladder, bone, lung, and ovaries while overestimate for liver, muscle, and spleen. In this study, the absorbed dose from

Table 4: The human absorbed dose estimation by MIRD schema and MCNP simulation

Target organ	Dose by MIRD (mGy/MBq)	Dose by MCNP (mGy/MBq)	Relative difference
Adernals	1.555E-02	1.798E-02	1.353E-01
Bladder wall	1.212E-03	1.322E-03	8.311E-02
Bone (total)	9.732E-03	1.706E-02	4.296E-01
GI (stomach wall)	8.177E-03	7.040E-03	1.615E-01
GI (ULI wall)	7.026E-03	6.585E-03	6.700E-02
Kidneys	3.938E-02	3.979E-02	1.040E-02
Liver	1.351E+00	1.266E+00	6.766E-02
Lungs	7.346E-01	8.081E-01	9.094E-02
Muscles	1.360E-02	1.160E-02	1.726E-01
Ovaries	1.671E-03	2.430E-03	3.122E-01
Pancreas	1.638E-02	1.619E-02	1.142E-02
Skin	2.280E-03	2.521E-03	9.533E-02
Spleen	1.031E+00	8.347E-01	2.356E-01
Testes	6.294E-04	4.736E-04	3.289E-01
Thyroid	1.841E-03	3.428E-03	4.629E-01
Uterus (nongravid)	1.771E-03	2.223E-03	2.034E-01

MIRD: Medical Internal Radiation Dosimetry, MCNP: Monte Carlo N-Particle Transport Code, GI: Gastrointestinal, ULT: Upper Large Intestine

PAMAM encapsulated Yb-175 estimated by MCNPX for liver, lung, spleen, kidney, and bone is 1.266, 8.081E-01, 8.347E-01, 3.979E-02, and 1.706E-02 mGy/MBq, respectively. As the simulation by MCNP is similar to the realistic situation and covers all the environmental scattering effects, where no scattering calculation in MIRD method is performed, this may be the reason of variation of the values that were estimated by MIRD and MCNP simulation.

Figure 6 shows the plot of source data by MCNPX plotter the various densities of points is because of the view plane of geometry. These view planes is X-Z plane, and for example, in the middle part of the abdomen the spleen, liver, and muscles are overlapped.

Conclusion

The clinical application of β-emitter radiopharmaceuticals requires quantitative data on both biodistribution and the

radiation dose of the desired radiopharmaceutical, and the aim of this study was to estimate the absorbed dose from intravenously injection of a newly performed nano radiopharmaceutical by PAMAM encapsulated ^{175}Yb to humans' organs. Owing to the stability of PAMAM encapsulated ^{175}Yb and the size of nanoparticle the concentrations are mostly in the liver and lungs.

Compiling data on the dosimetry of radiopharmaceutical inevitably leads to collecting reliable data for dosimetry in nuclear medicine. State-of-the-art dosimetry depends on the duration of the biokinetics of the radiopharmaceutical and a calculation of residence times including an analysis of the errors associated with the respective calculation and this aspect of PAMAM encapsulated ^{175}Yb for application in nuclear medicine was performed in this study.

The results showed that ^{175}Yb-PAMAM nano radiopharmaceutical has the potential of application for liver and lung tumors although further investigation in higher animals for obtaining more precise result in estimating the human's absorbed dose is necessary.

Financial support and sponsorship

Nil.

Conflicts of interest

There are no conflicts of interest.

References

1. Esumi K, Suzuki A, Yamahira A, Torigoe K. Role of poly (amidoamine) dendrimers for preparing nanoparticles of gold, platinum, and silver. Langmuir 2000;16:2604-8.
2. Majoros IJ, Thomas TP, Mehta CB, Baker JR Jr. Poly (amidoamine) dendrimer-based multifunctional engineered nanodevice for cancer therapy. J Med Chem 2005;48:5892-9.
3. Patri AK, Majoros IJ, Baker JR. Dendritic polymer macromolecular carriers for drug delivery. Curr Opin Chem Biol 2002;6:466-71.
4. Stiriba SE, Frey H, Haag R. Dendritic polymers in biomedical applications: From potential to clinical use in diagnostics and therapy. Angew Chem Int Ed Engl 2002;41:1329-34.
5. Ting G, Chang CH, Wang HE, Lee TW. Nanotargeted radionuclides for cancer nuclear imaging and internal radiotherapy. J Biomed Biotechnol 2010;2010. pii: 953537.
6. Baker JR Jr. Dendrimer-based nanoparticles for cancer therapy. Hematology Am Soc Hematol Educ Program 2009;2009:708-19.
7. Ting G, Chang CH, Wang HE. Cancer nanotargeted radiopharmaceuticals for tumor imaging and therapy. Anticancer Res 2009;29:4107-18.
8. Bult W, Kroeze SG, Elschot M, Seevinck PR, Beekman FJ, de Jong HW, *et al.* Intratumoral administration of holmium-166 acetylacetonate microspheres: Antitumor efficacy and feasibility of multimodality imaging in renal cancer. PLoS One 2013;8:e52178.
9. Diener MD, Alford JM, Kennel SJ, Mirzadeh S. (212) Pb@C (60) and its water-soluble derivatives: Synthesis, stability, and suitability for radioimmunotherapy. J Am Chem Soc 2007;129:5131-8.
10. Shultz MD, Duchamp JC, Wilson JD, Shu CY, Ge J, Zhang J, *et al.* Encapsulation of a radiolabeled cluster inside a fullerene cage, (177) Lu(x)Lu((3-x))N@C(80): An interleukin-13-conjugated radiolabeled metallofullerene platform. J Am Chem Soc 2010;132:4980-1.
11. Aghaei-Amirkhizi N, Moghaddam-Banaem L, Athari-Allaf M, Sadjadi S, Johari-Daha F. Development of dendrimer encapsulated radio-ytterbium and biodistributionin tumor bearing mice. IEEE Trans Nanobioscience 2016;15:549-54.
12. Mirzadeh S, Mausner LF, Garland MA. Reactor-Produced Medical Radionuclides. In: Vértes A, Nagy S, Klencsár Z, Lovas RG, Rösch F. (eds) Handbook of Nuclear Chemistry. Springer, Boston, MA; 2011.
13. Safarzadeh L, Ghannadi-Maragheh M, Anvari A, Aghamiri SM, Shirvani-Arani S, Bahrami-Samani A. Production, radiolabeling and biodistribution studies of 175Yb-DOTMP as bone pain palliation. Iran J Pharm Sci 2012;8:135-41.
14. Scott RW, Ye H, Henriquez RR, Crooks RM. Synthesis, characterization, and stability of dendrimer-encapsulated palladium nanoparticles. Chem Mater 2003;15:3873-8.
15. Harrison J, Day P. Radiation doses and risks from internal emitters. J Radiol Prot 2008;28:137-59.
16. Sgouros G. Dosimetry of internal emitters. J Nucl Med 2005;46 Suppl 1:18S-27S.
17. Solberg TD, DeMarco JJ, Chetty IJ, Mesa AV, Cagnon CH, Li AN, *et al*. A review of radiation dosimetry applications using the MCNP Monte Carlo code. Radiochimica Acta 2001;89:337-55.
18. Strand SE, Jönsson BA, Ljungberg M, Tennvall J. Radioimmunotherapy dosimetry – A review. Acta Oncol 1993;32:807-17.
19. Eberlein U, Bröer JH, Vandevoorde C, Santos P, Bardiès M, Bacher K, *et al.* Biokinetics and dosimetry of commonly used radiopharmaceuticals in diagnostic nuclear medicine – A review. Eur J Nucl Med Mol Imaging 2011;38:2269-81.
20. DeNardo GL, Raventos A, Hines HH, Scheibe PO, Macey DJ, Hays MT, *et al.* Requirements for a treatment planning system for radioimmunotherapy. Int J Radiat Oncol Biol Phys 1985;11:335-48.
21. Erwin WD, Groch MW, Macey DJ, DeNardo GL, DeNardo SJ, Shen S, *et al.* A radioimmunoimaging and MIRD dosimetry treatment planning program for radioimmunotherapy. Nucl Med Biol 1996;23:525-32.
22. Fisher DR. Radiation dosimetry for radioimmunotherapy. An overview of current capabilities and limitations. Cancer 1994;73:905-11.
23. Yoriyaz H, Stabin MG, dos Santos A. Monte carlo MCNP-4B-based absorbed dose distribution estimates for patient-specific dosimetry. J Nucl Med 2001;42:662-9.
24. Biological Council. Guidelines on the use of Living Animals in Scientific Investigations. Biological Council; 1987.
25. Stabin MG. Fundamentals of Nuclear Medicine Dosimetry. New York, USA: Springer Science & Business Media; 2008.
26. Valentin J. Basic anatomical and physiological data for use in radiological protection: reference values: ICRP Publication 89. Ann ICRP 2002;32:1-277.
27. Stabin MG. MIRDOSE: Personal computer software for internal dose assessment in nuclear medicine. J Nucl Med 1996;37:538-46.
28. Snyder W, Ford M, Warner G, Watson S. MIRD Pamphlet no. 11. New York: The Society of Nuclear Medicine; 1975. p. 92-3.
29. Blanco E, Shen H, Ferrari M. Principles of nanoparticle design for overcoming biological barriers to drug delivery. Nat Biotechnol 2015;33:941-51.
30. He C, Hu Y, Yin L, Tang C, Yin C. Effects of particle size and surface charge on cellular uptake and biodistribution of polymeric nanoparticles. Biomaterials 2010;31:3657-66.
31. Kulkarni SA, Feng SS. Effects of particle size and surface modification on cellular uptake and biodistribution of polymeric nanoparticles for drug delivery. Pharm Res 2013;30:2512-22.
32. Mohanraj V, Chen Y. Nanoparticles – A review. Trop J Pharm Res 2007;5:561-73.